Western University
Scholarship@Western

Kinesiology Publications | Kinesiology School

8-19-2016

Effects of aging and coronary artery disease on sympathetic neural recruitment strategies during end-inspiratory and end-expiratory apnea

Mark B. Badrov
Western University

Sophie Lalande
Western University

T Dylan Olver
Western University

Neville Suskin
Western University

J Kevin Shoemaker
Western University, kshoemak@uwo.ca

Follow this and additional works at: https://ir.lib.uwo.ca/kinpub

 Part of the Kinesiology Commons

Citation of this paper:
Badrov, Mark B.; Lalande, Sophie; Olver, T Dylan; Suskin, Neville; and Shoemaker, J Kevin, "Effects of aging and coronary artery disease on sympathetic neural recruitment strategies during end-inspiratory and end-expiratory apnea" (2016). *Kinesiology Publications*. 49.
https://ir.lib.uwo.ca/kinpub/49

Am J Physiol Heart Circ Physiol 311: H1040–H1050, 2016.
First published August 19, 2016; doi:10.1152/ajpheart.00334.2016.

Effects of aging and coronary artery disease on sympathetic neural recruitment strategies during end-inspiratory and end-expiratory apnea

Mark B. Badrov,[1] Sophie Lalande,[1,2] T. Dylan Olver,[1] Neville Suskin,[3,4] and J. Kevin Shoemaker[1,5]

[1]*School of Kinesiology, Western University, London, Ontario, Canada;* [2]*Department of Kinesiology, University of Toledo, Toledo, Ohio;* [3]*Cardiac Rehabilitation and Secondary Prevention Program of St. Joseph's Health Care London, London, Ontario, Canada;* [4]*Department of Medicine (Cardiology) and Program of Experimental Medicine, Western University, London, Ontario, Canada; and* [5]*Department of Physiology and Pharmacology, Western University, London, Ontario, Canada*

Submitted 2 May 2016; accepted in final form 17 August 2016

Badrov MB, Lalande S, Olver TD, Suskin N, Shoemaker JK. Effects of aging and coronary artery disease on sympathetic neural recruitment strategies during end-inspiratory and end-expiratory apnea. *Am J Physiol Heart Circ Physiol* 311: H1040–H1050, 2016. First published August 19, 2016; doi:10.1152/ajpheart.00334.2016.—In response to acute physiological stress, the sympathetic nervous system modifies neural outflow through increased firing frequency of lower-threshold axons, recruitment of latent subpopulations of higher-threshold axons, and/or acute modifications of synaptic delays. Aging and coronary artery disease (CAD) often modify efferent muscle sympathetic nerve activity (MSNA). Therefore, we investigated whether CAD ($n = 14$; 61 ± 10 yr) and/or healthy aging without CAD (OH; $n = 14$; 59 ± 9 yr) modified these recruitment strategies that normally are observed in young healthy (YH; $n = 14$; 25 ± 3 yr) individuals. MSNA (microneurography) was measured at baseline and during maximal voluntary end-inspiratory (EI) and end-expiratory (EE) apneas. Action potential (AP) patterns were studied using a novel AP analysis technique. AP frequency increased in all groups during both EI- and EE-apnea (all $P < 0.05$). The mean AP content per integrated burst increased during EI- and EE-apnea in YH (EI: $\Delta 6 \pm 4$ APs/burst; EE: $\Delta 10 \pm 6$ APs/burst; both $P < 0.01$) and OH (EI: $\Delta 3 \pm 3$ APs/burst; EE: $\Delta 4 \pm 5$ APs/burst; both $P < 0.01$), but not in CAD (EI: $\Delta 1 \pm 3$ APs/burst; EE: $\Delta 2 \pm 3$ APs/burst; both $P =$ NS). When APs were binned into "clusters" according to peak-to-peak amplitude, total clusters increased during EI- and EE-apnea in YH (EI: $\Delta 5 \pm 2$; EE: $\Delta 6 \pm 4$; both $P < 0.01$), during EI-apnea only in OH (EI: $\Delta 1 \pm 2$; $P < 0.01$; EE: $\Delta 1 \pm 2$; $P =$ NS), and neither apnea in CAD (EI: $\Delta -2 \pm 2$; EE: $\Delta -1 \pm 2$; both $P =$ NS). In all groups, the AP cluster size-latency profile was shifted downwards for every corresponding cluster during EI- and EE-apnea (all $P < 0.01$). As such, inherent dysregulation exists within the central features of apnea-related sympathetic outflow in aging and CAD.

coronary artery disease; sympathetic nervous system; aging; sympathetic neural recruitment patterns; apnea

NEW & NOTEWORTHY

The current data provide the first multiunit evidence that the sympathetic dysregulation observed under resting conditions with increasing age and cardiovascular disease extends to the neural recruitment strategies employed by the sympathetic nervous system in response to an acute homeostatic challenge.

SYMPATHETIC NERVOUS SYSTEM dysregulation represents a hallmark of increasing age and cardiovascular disease. This dysregulation has been well-studied at rest, where aging and cardiovascular disease are characterized by a net elevation in baseline sympathetic outflow (14, 35), which contributes to numerous deleterious consequences, including cardiac and vascular damage and remodeling, cardiac dysrhythmias, and an elevated risk of mortality (4, 13, 29). However, the mechanisms involved in aberrant sympathetic control with aging and cardiovascular disease, such as the distinct features of central recruitment strategies, are not known.

Normally, sympathetic neural control involves central integration of sensory and cortical/subcortical signals within the brain stem and spinal cord (3), synapses at the sympathetic ganglia (18), efferent postganglionic nerve traffic, neurotransmitter release, and the subsequent vascular effect at the end organ (36). These elements introduce multiple sites of control in which sympathetic outflow can be coded and modified in response to acute physiological perturbation. Data from direct single- and multifiber recordings of central sympathetic outflow in young healthy individuals indicate that the sympathetic nervous system has options to increase the firing frequency and probability of low-threshold axons (22, 31), recruit latent subpopulations of higher-threshold and faster conducting axons (2, 39), as well as acutely modify synaptic delays and/or central processing times (2, 32). These patterns illustrate unique properties of the central nervous system to fine-tune autonomic homeostatic control.

Whether these neural coding strategies are affected by increasing age and cardiovascular pathology normally associated with advancing age remains uncertain. While recordings from single muscle vasoconstrictor axons reveal an increased firing probability and frequency of single units in cardiovascular disease (15, 21), the typical observation that a given neuron will fire usually only once per sympathetic burst at rest appears unchanged in congestive heart failure with reduced left ventricular ejection fraction (LVEF) (21, 23). Conversely, within-burst firing frequency of single axons at baseline is increased in other states of chronic sympathetic arousal, such as obstructive sleep apnea (10) and chronic obstructive pulmonary disease (1), as well as in response to an acute physiological challenge (9, 22, 27). However, information regarding the several recruitment strategies available (i.e., recruitment of new axons) to the sympathetic nervous system cannot be extracted from single-unit recordings, but requires a multiunit analysis model. Using multifiber recordings, we have documented recruitment of new subpopulations of larger axons (2, 5, 39), as well as modifiable synaptic delays (2), in response to voluntary apnea-induced sympathoexcitation in young healthy individuals. However, the ability to recruit latent neuronal subpopulations may be diminished with healthy aging and cardiovascular disease (24, 25).

Address for reprint requests and other correspondence: J. K. Shoemaker, School of Kinesiology, Western Univ., 1151 Richmond St., London, Ontario, Canada (e-mail: kshoemak@uwo.ca).

0363-6135/16 Copyright © 2016 the American Physiological Society

Downloaded from journals.physiology.org/journal/ajpheart at Univ Western Ontario (129.100.136.165) on September 1, 2022.

Therefore, the current study examined the hypothesis that cardiovascular disease impairs sympathetic neural recruitment. Coronary artery disease (CAD) patients with preserved LVEF completed maximal voluntary apneas, which served as a stimulus for sympathoexcitation, and the response was compared with that of young healthy and older healthy individuals to account for the concurrent effect of age.

METHODS

Participants. Forty-two individuals participated in the current investigation after providing informed written consent. Participants comprised three groups: *1*) young healthy individuals (YH; $n = 14$, 5 females), *2*) older healthy individuals (OH; $n = 14$; 6 females), and *3*) CAD patients (CAD; $n = 14$, 3 females). Participant characteristics are summarized in Table 1. YH and OH participants were nonsmokers, free of overt disease, and nonmedicated. CAD patients included those who were discharged from hospital following an acute ST elevation ($n = 7$) or non-ST elevation ($n = 7$) myocardial infarction (MI) as documented by their attending physician. In all instances, patients presented with their first MI. Eleven patients underwent percutaneous coronary intervention and four underwent coronary artery bypass grafting surgery. No CAD patients had a history of congestive heart failure, renal insufficiency, or diabetes mellitus, and all had preserved LVEF at the time of study. Although all patients were on antihypertensive medications, all presented with resting blood pressures within the normal range (i.e., <140/90 mmHg). Six patients were former or current smokers at the time of study. On average, testing took place 67 ± 37 days following hospital discharge. Medication use in the CAD patients included beta-blockers ($n = 13$; 93%), angiotensin converting enzyme inhibitors ($n = 13$; 93%), calcium channel blockers ($n = 3$; 21%), diuretics ($n = 1$; 8%), statins ($n = 13$; 93%), and anti-platelets, including aspirin ($n = 14$; 100%). All experimental protocols were approved by the Health Sciences Research Ethics Board at Western University.

Experimental protocols. Participants arrived for testing having fasted and abstained from caffeine and alcohol for 12 h, and vigorous exercise for 24 h. Data were collected in the supine position during *1*) a 1-min baseline period and a subsequent end-inspiratory (EI) apnea of maximal voluntary duration, and *2*) a 1-min baseline period and a subsequent end-expiratory (EE) apnea of maximal voluntary duration. Both EI- and EE-apnea were repeated twice, with each trial separated by 3 min of rest. EI- and EE-apnea were used as stimuli to increase muscle sympathetic nerve activity (MSNA) in order to study the neural recruitment strategies employed by the sympathetic nervous system during reflex-mediated sympathoexcitation. Both EI- and EE-apnea elicit marked increases in sympathetic outflow, albeit through different mechanisms. Voluntary EI-apnea increases MSNA through a variety of factors including unloading of the baroreceptors, chemoreflex activation, and an increased central drive-to-breathe (12, 17, 37, 38). On the other hand, EE-apnea increases MSNA predominantly through chemoreflex stimulation, as well as a lack of ventilatory restraint on sympathetic outflow, and increased central drive-to-breathe (17, 37, 38).

Table 1. *Participant characteristics*

	YH	OH	CAD
Age, yr	25 ± 3	59 ± 9*	61 ± 10*
Height, cm	173 ± 8	168 ± 7	169 ± 9
Weight, kg	74 ± 13	68 ± 11	86 ± 15*†
Body mass index, kg/m^2	25 ± 4	25 ± 2	30 ± 5*†
Systolic BP, mmHg	113 ± 13	121 ± 16	120 ± 21
Diastolic BP, mmHg	69 ± 10	74 ± 10	66 ± 9
HR, beats/min	63 ± 6	58 ± 8	60 ± 8
CO, l/min	6.2 ± 1.3	5.4 ± 1.4	6.2 ± 1.2
TPR, mmHg·l^{-1}·min	14 ± 4	18 ± 7	14 ± 4
LVEF, %	68 ± 4	68 ± 4	61 ± 9
Burst frequency, bursts/min	18 ± 8	34 ± 9*	41 ± 7*
Burst incidence, bursts/100 hb	29 ± 13	58 ± 14*	69 ± 11*
Total MSNA, AU	989 ± 380	1,916 ± 540*	2,331 ± 372*
Glucose, mmol/l	5.1 ± 0.6	5.2 ± 0.4	5.6 ± 0.7
Total cholesterol, mmol/l	3.6 ± 1.0	4.3 ± 0.6	3.2 ± 0.6†
HDL cholesterol, mmol/l	1.2 ± 0.2	1.5 ± 0.3	1.0 ± 0.1†
LDL cholesterol, mmol/l	2.0 ± 1.0	2.4 ± 0.6	1.7 ± 0.5
Triglycerides, mmol/l	0.9 ± 0.3	0.9 ± 0.4	1.0 ± 0.3
HbA1C, %	5.4 ± 0.2	5.7 ± 0.2*	5.8 ± 0.3*

Values are the mean of the two baseline periods (mean ± SD). YH, young healthy; OH, older healthy; CAD, coronary artery disease; BP, blood pressure; HR, heart rate; CO, cardiac output; TPR, total peripheral resistance; LVEF, left ventricular ejection fraction; hb, heart beats; MSNA, muscle sympathetic nerve activity; AU, arbitrary units. HDL, high-density lipoprotein; LDL, low-density lipoprotein; HbA1C, hemoglobin A1C. *Significantly different from YH, $P < 0.01$; †Significantly different from OH, $P < 0.01$.

Experimental measures. Sympathetic neural recordings were obtained in the right peroneal nerve by microneurography, using standard procedures originally defined by Hagbarth and Vallbo (16) and used frequently in our hands (2, 31, 39) (662C-3; Bioengineering of University of Iowa, Iowa City, IA). Blood pressure was obtained throughout the experimental protocol using finger photoplethysmography (Finometer; Finapres Medical Systems, Amsterdam, The Netherlands), which was calibrated to manual sphygmomanometry. Heart rate (HR) was calculated from a standard three-lead electrocardiogram. Stroke volume (SV) and cardiac output (CO) were acquired using the Finometer Modelflow algorithm, and total peripheral resistance (TPR) was calculated as the quotient of mean arterial pressure (MAP) and CO. All data were collected and analyzed offline using LabChart6 and PowerLab (ADInstruments, Colorado Springs, CO).

Data analysis. For both the EI- and EE-apnea protocols, data were analyzed for the 1-min baseline period and during the second half of maximal voluntary apnea. MSNA was analyzed from the integrated neurogram and from our technique to detect and extract action potentials (APs) from the filtered raw MSNA signal (30). Integrated MSNA was quantified using burst frequency and burst incidence [bursts per minute and bursts per 100 heart beats (hb), respectively]. Furthermore, burst amplitude (normalized to the largest burst at baseline, which was given a value of 100) and total MSNA (product of normalized burst amplitude and burst frequency) were determined.

Individual APs were extracted from the filtered raw MSNA signal using wavelet-based methodology, as first reported by others (6, 8), and modified in our hands (30). Our approach, described in detail elsewhere (2, 30), uses a continuous wavelet transform constructed from real postganglionic sympathetic APs (30), that extracts APs at their point of occurrence, and classifies them according to their peak-to-peak amplitude into clusters (i.e., bins) of similarly-sized APs using Scott's rule (34). To enable investigation into whether recruitment of new, larger AP clusters occurred during apnea, a secondary analysis stage was introduced whereby cluster characteristics were manipulated within each participant so that minimum bin width, maximum bin center, and the total number of bins would be identical across conditions. Therefore, corresponding clusters at baseline and apnea contain APs with similar peak-to-peak amplitudes, while additional clusters during apnea represent recruitment of latent subpopulations of larger-sized axons (i.e., not present at baseline).

AP variables were quantified using AP frequency and AP incidence (APs per minute and APs per 100 hb, respectively), as well as the mean AP content per integrated sympathetic burst. Furthermore, the number of total AP clusters and the number of active clusters per burst are presented. AP cluster latency was calculated as the average latency of all APs present within that cluster (as measured by the time delay between the R-wave of the electrocardiogram of the preceding cardiac cycle and the negative peak of the AP waveform). To adjust for the impact of interindividual variations in total cluster number on calculations of changes in AP cluster latency, the number of total clusters

Downloaded from journals.physiology.org/journal/ajpheart at Univ Western Ontario (129.100.136.165) on September 1, 2022.

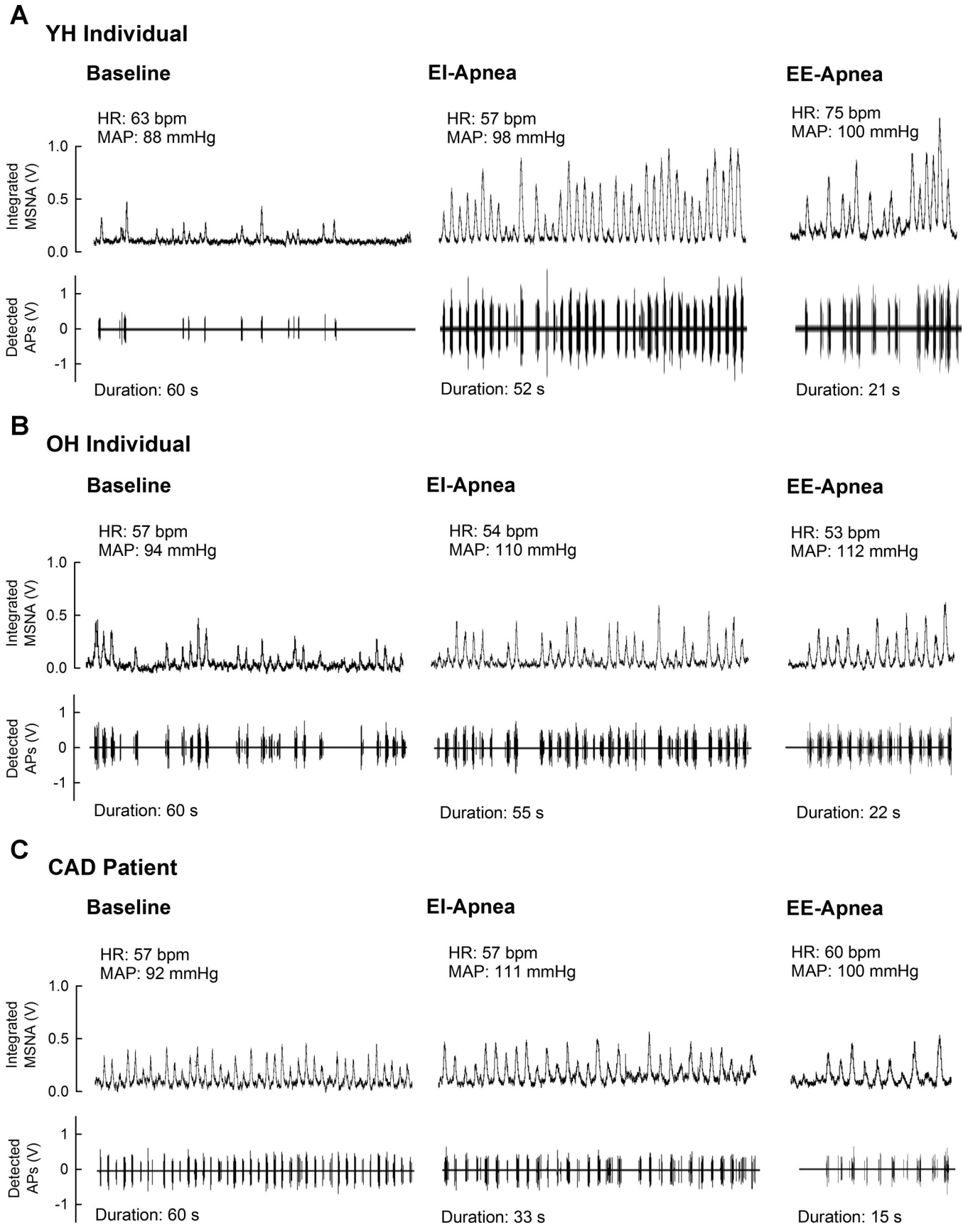

Downloaded from journals.physiology.org/journal/ajpheart at Univ Western Ontario (129.100.136.165) on September 1, 2022.

Table 2. *Hemodynamic responses to end-inspiratory and end-expiratory apnea*

	YH	OH	CAD
End-inspiratory apnea			
Δ MAP, mmHg	9 ± 5	6 ± 8	8 ± 8
Δ HR, beats/min	2 ± 9	3 ± 10	2 ± 4
Δ SV, ml	−20 ± 13	−22 ± 12	−17 ± 17
Δ CO, l/min	−1.1 ± 1.0	−1.2 ± 0.9	−1.0 ± 0.9
Δ TPR, mmHg·l^{-1}·min	5 ± 3	7 ± 5	5 ± 3
End-expiratory apnea			
Δ MAP, mmHg	11 ± 4	8 ± 6	7 ± 5
Δ HR, beats/min	4 ± 11	0 ± 9	0 ± 3
Δ SV, ml	−4 ± 10	−12 ± 8	−7 ± 10
Δ CO, l/min	0.1 ± 0.5	−0.6 ± 0.6	−0.5 ± 0.5
Δ TPR, mmHg·l^{-1}·min	2 ± 2	5 ± 4	3 ± 2

Values are mean ± SD. YH, young healthy; OH, older healthy; CAD, coronary artery disease; MAP, mean arterial pressure; HR, heart rate; SV, stroke volume; CO, cardiac output; TPR, total peripheral resistance.

Table 3. *Integrated MSNA and action potential indexes at baseline and during maximal end-inspiratory apnea*

	Baseline	EI-Apnea	Δ
Integrated MSNA indexes			
Burst frequency, bursts/min			
YH	17 ± 8	41 ± 8†	25 ± 10
OH	35 ± 9*	51 ± 11†	16 ± 7‡
CAD	41 ± 7*	53 ± 8†	11 ± 8‡
Burst incidence, bursts/100 hb			
YH	27 ± 14	65 ± 15†	38 ± 18
OH	60 ± 14*	82 ± 13†	22 ± 14‡
CAD	70 ± 10*	88 ± 6†	18 ± 10‡
Burst amplitude, AU			
YH	57 ± 8	100 ± 25†	43 ± 20
OH	57 ± 6	80 ± 16†	24 ± 15‡
CAD	57 ± 5	69 ± 13†	12 ± 12‡
Total MSNA, AU			
YH	908 ± 389	4,144 ± 1379†	3,236 ± 1476
OH	2,002 ± 614*	4,077 ± 1211†	2,075 ± 1113‡
CAD	2,357 ± 415*	3,624 ± 811†	1,267 ± 700‡
Action potential indexes			
AP frequency, spikes/min			
YH	189 ± 222	691 ± 480†	502 ± 356
OH	372 ± 226	698 ± 402†	326 ± 223
CAD	410 ± 180	584 ± 279†	174 ± 196‡
AP incidence, spikes/100 hb			
YH	307 ± 353	1,081 ± 757†	774 ± 581
OH	614 ± 343	1,136 ± 681†	522 ± 461
CAD	694 ± 302	968 ± 465†	274 ± 305‡

Values are mean ± SD. EI, end-inspiratory; MSNA, muscle sympathetic nerve activity; YH, young healthy; OH, older healthy; CAD, coronary artery disease; hb, heart beats; AU, arbitrary units; AP, action potential. *Significantly different from YH baseline value, $P < 0.01$; †Significantly different from baseline, $P < 0.01$; ‡Significantly different from YH delta value, $P < 0.01$.

was normalized to 10 bins (i.e., 10% ranges of the largest detected cluster, which was given a value of 100%) for this analysis step, as described previously (2).

Statistical analysis. Mixed model ANOVAs (SigmaPlot 12.0; Systat Software, San Jose, CA) assessed the effect of group vs. time (baseline vs. EI-apnea; baseline vs. EE-apnea) on MSNA and hemodynamic variables. Bonferroni-corrected post hoc procedures were used to evaluate specific differences between means. Regression analyses were used to determine specific relationships between variables when applicable. For the EE-apnea protocol, six participants (YH, $n = 2$; OH, $n = 2$; CAD, $n = 2$) were excluded as their MSNA signal was obscured by motor-unit activation and/or a signal-to-noise ratio (SNR) that was too poor to allow for adequate AP analysis. Statistical significance was set at $P < 0.05$, and all data are means ± SD, unless otherwise stated.

RESULTS

As noted above, some MSNA recordings lacked appropriate SNR or were contaminated by motor-unit activation. Also, variations exist between individuals in the duration of apnea, as well as within individuals in terms of the response and duration to repeated apneas. To address these issues, Bland-Altman analyses assessed the agreement between the first and second EI- and EE-apneas for all MSNA and AP variables. Participants with SNR >3.7 (i.e., to allow for adequate AP detection) for both apneas were included in the analysis (EI-apnea, $n = 33$; EE-apnea, $n = 21$). Briefly, while the second EI- and EE-apnea were of longer duration (EI-apnea: 41 ± 17 vs. 36 ± 17 s; EE-apnea: 21 ± 10 vs. 19 ± 10 s; both $P < 0.05$), no differences existed between the first and second sympathetic response to either EI- or EE-apnea (all $P =$ NS), and all MSNA and AP variables were without significant fixed or proportional bias (EI-apnea: total MSNA, 127 ± 139, mean difference ± SE; APs/burst, 0.6 ± 0.5; clusters/burst, 0.1 ± 0.1; total clusters, 0.2 ± 0.5; EE-apnea: total MSNA, −474 ± 315; APs/burst, 0.6 ± 0.7; clusters/burst, 0.3 ± 0.2; total clusters, −0.5 ± 0.6). With no within-individual differences between the first and second apnea, the average of the two EI- and two EE-apneas were used in the final analysis. Reexamination of results with removal of statistical outliers (i.e., those individuals with data points that were more than 1.5 interquartile ranges below the first quartile or above the third quartile) did not significantly alter the results; therefore, data from these individuals were retained in the final analysis (40). Finally, the mean SNR in the current study was 4.1 ± 0.5, which is expected to produce a correct detection rate of >90% and a false positive rate of <3% (30).

Figure 1 displays representative recordings of the integrated MSNA neurogram and detected APs from one YH individual, one OH individual, and one CAD patient at baseline and during EI-apnea and EE-apnea.

Baseline vs. end-inspiratory apnea. The duration of the second half of EI-apnea was 46 ± 17 s (range 27 to 78 s) in YH, 35 ± 15 s (range 15 to 70 s) in OH, and 28 ± 6 s (range 19 to 44 s) in CAD patients. In a pointwise contrast, CAD patients had a lower EI-apnea duration compared with YH ($P < 0.01$). MAP, HR, and TPR exhibited effects of time, whereby each increased during EI-apnea, while reductions in SV and CO occurred (all $P < 0.05$; Table 2); however, no group differences existed in the hemodynamic response to EI-apnea (all $P =$ NS).

Fig. 1. Representative recordings of the integrated muscle sympathetic nerve activity (MSNA) neurogram and detected action potentials (APs) from one young healthy (YH) individual (*A*), one older healthy (OH) individual (*B*), and one coronary artery disease (CAD) patient (*C*) at baseline and during end-inspiratory (EI) and end-expiratory (EE) apnea. HR, heart rate; MAP, mean arterial pressure; bpm, beats per minute.

Downloaded from journals.physiology.org/journal/ajpheart at Univ Western Ontario (129.100.136.165) on September 1, 2022.

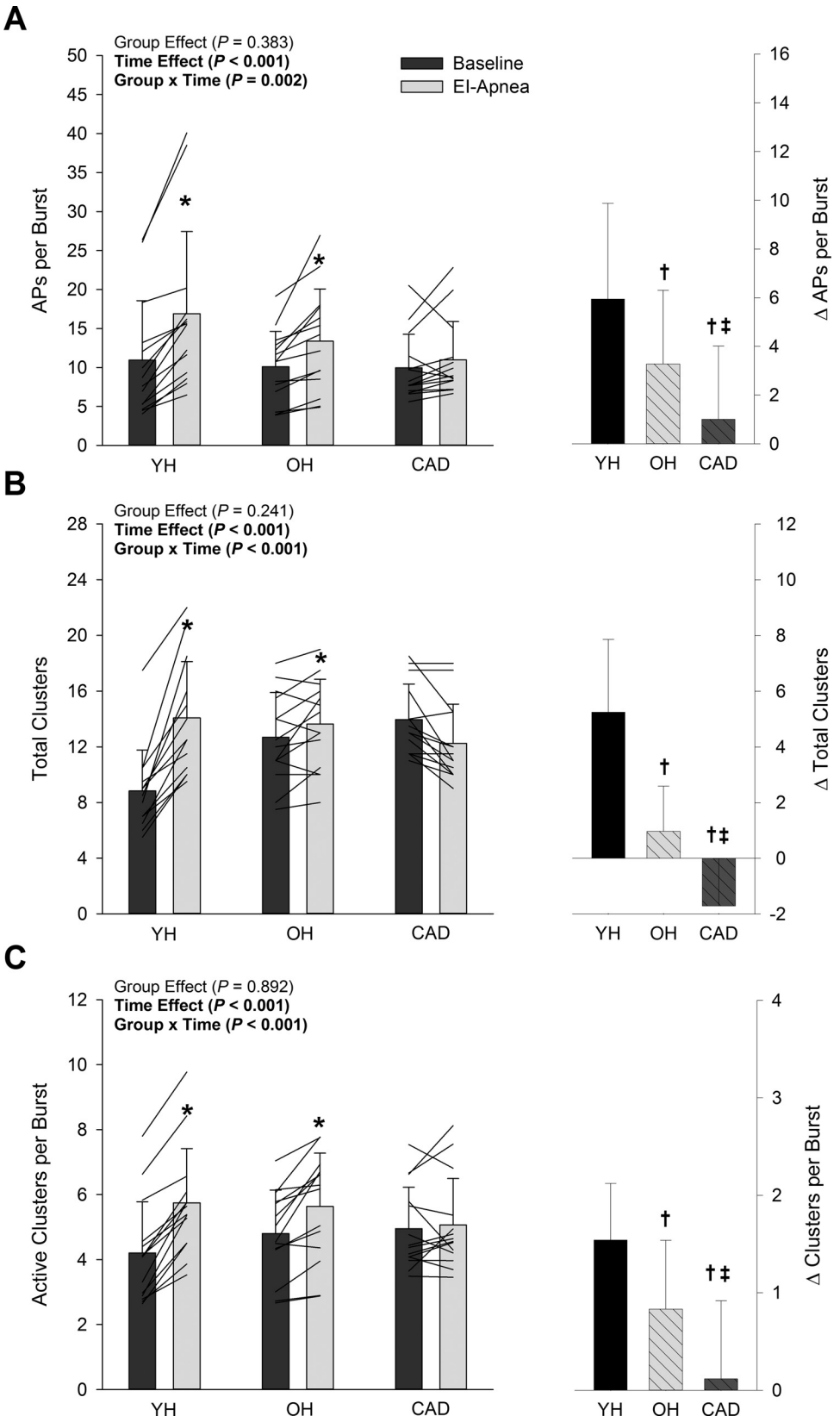

Fig. 2. Action potential (AP) content per burst (*A*), total clusters (*B*), and active clusters per burst (*C*) in young healthy (YH), older healthy (OH), and coronary artery disease (CAD) patients at baseline and during end-inspiratory (EI) apnea (left panel; individual lines represent individual data). Right panel represents the absolute delta change from baseline to EI-apnea. *Significantly different from baseline, $P < 0.01$. †Significantly different from YH, $P < 0.01$. ‡Significantly different from OH, $P < 0.01$.

Downloaded from journals.physiology.org/journal/ajpheart at Univ Western Ontario (129.100.136.165) on September 1, 2022.

Table 3 outlines the integrated MSNA and AP indexes during EI-apnea and their relative baseline values. Compared with YH, baseline burst frequency and burst incidence were higher in OH and CAD (all $P < 0.01$), but no differences were observed between OH and CAD (P = NS). Compared with baseline, all integrated MSNA variables increased during EI-apnea in all groups (all $P < 0.01$). However, compared with YH, the change in integrated MSNA was blunted in OH and CAD (all $P < 0.01$), with no differences between OH and CAD (P = NS). Whereas EI-apnea resulted in increased AP frequency and AP incidence in all groups (all $P < 0.01$), CAD patients had a reduced ability to increase AP frequency and AP incidence compared with YH (both $P < 0.01$). No differences in the AP frequency and AP incidence response existed between YH and OH (P = NS) or OH and CAD (P = NS).

Compared with baseline, the mean AP content per burst increased during EI-apnea in YH (11 ± 8 to 17 ± 11 APs/burst; $P < 0.01$) and OH (10 ± 5 to 13 ± 7 APs/burst; $P < 0.01$), while no change occurred in CAD patients (10 ± 4 to 11 ± 5 APs/burst; P = NS; Fig. 2*A*). The magnitude of response was reduced in both OH and CAD compared with YH ($P < 0.01$), and further reduced in CAD vs. OH ($P < 0.01$). When APs were binned according to their peak-to-peak amplitude, the number of total clusters of APs increased in YH (9 ± 3 to 14 ± 4 total clusters; $P < 0.01$) and OH (13 ± 3 to 14 ± 3 total clusters; $P < 0.01$) during EI-apnea, but not in CAD patients (14 ± 3 to 12 ± 3 total clusters; P = NS; Fig. 2*B*). The ability to recruit new clusters of APs was diminished in OH and CAD patients compared with YH ($P < 0.01$), and further decreased in CAD vs. OH ($P < 0.01$). Finally, the number of active clusters per burst increased during EI-apnea in YH (4 ± 2 to 6 ± 2 clusters/burst; $P < 0.01$) and OH (5 ± 1 to 6 ± 2 clusters/burst; $P < 0.01$), but not in CAD patients (5 ± 1 to 5 ± 1 clusters/burst; P = NS; Fig. 2*C*). The magnitude of change was lower in OH and CAD compared with YH (both $P < 0.01$), and further lowered in CAD compared with OH ($P < 0.01$). When all subjects were pooled, EI-apnea duration correlated poorly with the mean AP content per burst response ($r = 0.207$; P = NS) and the active clusters per burst response ($r = 0.277$; P = NS) to apnea. EI-apnea duration correlated moderately well with the total clusters response ($r = 0.553$; $P < 0.01$) to apnea; however, when accounting for age and incidence of CAD, EI-apnea duration no longer predicted the total clusters response to apnea (P = NS).

In all groups, at baseline (YH: $R^2 = 0.93$; OH: $R^2 = 0.90$; CAD: $R^2 = 0.77$; all $P < 0.01$) and during EI-apnea (YH: $R^2 = 0.97$; OH: $R^2 = 0.94$; CAD: $R^2 = 0.91$; all $P < 0.01$), a pattern emerged whereby AP cluster latency decreased as a function of normalized cluster number (i.e., as peak-to-peak AP cluster amplitude increased). The mean responses (Fig. 3) were fitted using an exponential function model at baseline and during EI-apnea. Interestingly, the cluster size-latency profile shifted downward for every corresponding cluster during apnea in YH (range −8 to −48 ms; mean −28 ± 15 ms; $P < 0.01$), OH (range −15 to −38 ms; mean −32 ± 7 ms; $P < 0.01$), and CAD patients (range −5 to −58 ms; mean −21 ± 17 ms; $P < 0.01$). No differences were found in the magnitude of change between groups (all P = NS).

Baseline vs. end-expiratory apnea. The duration of the second half of EE-apnea was 20 ± 10 s (range 12 to 47 s) in YH, 22 ± 11 s (range 8 to 45 s) in OH, and 16 ± 5 s (range 10 to 27 s) in CAD patients. No differences in duration were observed for EE-apnea between groups (P = NS). Both MAP and TPR exhibited effects of time, whereby values increased during EE-apnea; in contrast, reductions occurred

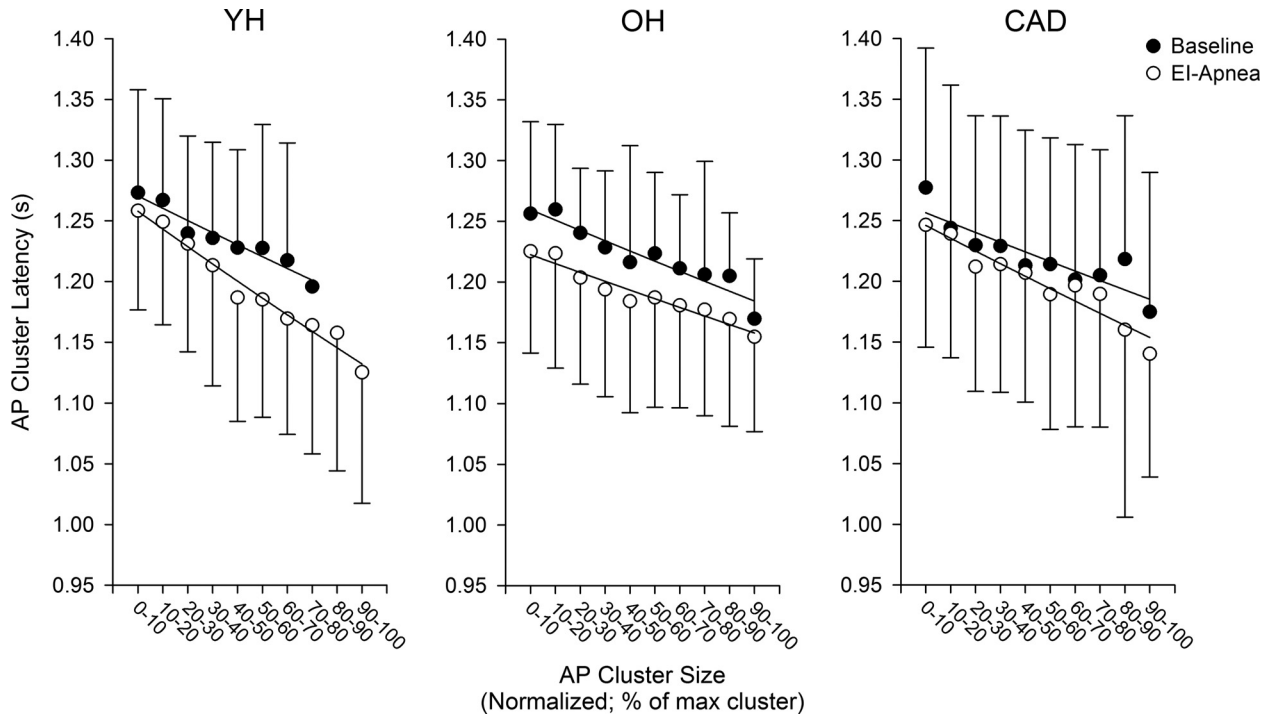

Fig. 3. Action potential (AP) cluster latency as a function of normalized cluster number (i.e., size) at baseline and during end-inspiratory (EI) apnea in young healthy (YH; left panel), older healthy (OH; middle panel), and coronary artery disease patients (CAD; right panel).

Downloaded from journals.physiology.org/journal/ajpheart at Univ Western Ontario (129.100.136.165) on September 1, 2022.

in SV and CO (all $P < 0.05$; Table 2). However, no group differences existed in the hemodynamic response to EE-apnea (all P = NS).

Table 4 outlines the integrated MSNA and AP indexes during EE-apnea and their relative baseline values. Once again, compared with YH, baseline burst frequency and burst incidence were higher in OH and CAD (all $P < 0.01$), but no differences were observed between OH and CAD (P = NS). Compared with baseline, all integrated MSNA variables increased during EE-apnea in all groups (all $P < 0.01$). However, compared with YH, the changes in burst frequency, burst amplitude, and total MSNA were blunted in OH and CAD (all $P < 0.01$), while the change in burst incidence was lower in CAD vs. YH ($P < 0.01$). No differences were found between OH and CAD for any integrated MSNA variable (all P = NS). Additionally, compared with baseline, EE-apnea resulted in increased AP frequency and AP incidence in all groups ($P < 0.05$); however, CAD patients had a decreased ability to increase AP frequency and AP incidence compared with YH ($P < 0.01$), while no differences existed between OH and CAD (P = NS).

Compared with baseline, the mean AP content per burst increased in YH (11 ± 6 to 20 ± 9 APs/burst; $P < 0.01$) and OH (11 ± 4 to 15 ± 8 APs/burst; $P < 0.01$) in response to EE-apnea, but was unchanged in CAD patients (11 ± 6 to 13 ± 6 APs/burst; P = NS; Fig. 4*A*). The change in the mean AP content per burst was lower in OH and CAD than in YH (both $P < 0.01$); however, no difference existed between OH and CAD (P = NS). When APs were binned according to their peak-to-peak amplitude, the number of total clusters of APs increased in YH (8 ± 4 to 14 ± 5 total clusters; $P < 0.01$), but was unchanged in both OH (12 ± 3 to 13 ± 4 total clusters; P = NS) and CAD patients (13 ± 4 to 12 ± 2 total clusters; P = NS; Fig. 4*B*). As such, the ability to recruit new clusters of APs was diminished in OH and CAD compared with YH (both $P < 0.01$). Finally, compared with baseline, the number of active clusters per burst increased during EE-apnea in YH (4 ± 2 to 6 ± 2 clusters/burst; $P < 0.01$) and OH (5 ± 1 to 6 ± 2 clusters/burst; $P < 0.01$), but not in CAD patients (5 ± 1 to 6 ± 1 clusters/burst; P = NS; Fig. 4*C*). The magnitude of change was lower in OH and CAD compared with YH ($P < 0.01$). When all subjects were pooled, EE-apnea duration correlated poorly with the mean AP content per burst response ($r = 0.029$; P = NS), the active clusters per burst response ($r = 0.117$; P = NS), as well as the total clusters response ($r = 0.297$; P = NS) to apnea.

Similar to EI-apnea, a pattern emerged during baseline (YH: $R^2 = 0.76$; OH: $R^2 = 0.85$; CAD: $R^2 = 0.88$; all $P < 0.01$) and EE-apnea (YH: $R^2 = 0.95$; OH: $R^2 = 0.97$; CAD: $R^2 = 0.87$; all $P < 0.01$), whereby AP cluster latency decreased as a function of normalized cluster number (i.e., as peak-to-peak AP cluster amplitude increased). The mean responses (Fig. 5) were fitted using an exponential function model at baseline and during EE-apnea. Once again, the cluster size-latency profile shifted downward for every corresponding cluster during apnea in YH (range −12 to −74 ms; mean −35 ± 23 ms; $P < 0.01$), OH (range 0 to −47 ms; mean −30 ± 14 ms; $P < 0.01$), and CAD patients (range −31 to −87 ms; mean: −59 ± 17 ms; $P < 0.01$). No differences were found in the magnitude of change between groups (all P = NS).

Table 4. *Integrated MSNA and action potential indexes at baseline and during maximal end-expiratory apnea*

	Baseline	EE-Apnea	Δ
Integrated MSNA indexes			
Burst frequency, bursts/min			
YH	19 ± 7	42 ± 12†	24 ± 13
OH	33 ± 9*	49 ± 11†	16 ± 6‡
CAD	41 ± 8*	51 ± 5†	10 ± 7‡
Burst incidence, bursts/100 hb			
YH	29 ± 11	64 ± 17†	34 ± 20
OH	56 ± 16*	83 ± 13†	27 ± 14
CAD	70 ± 11*	89 ± 5†	18 ± 13‡
Burst amplitude, AU			
YH	57 ± 7	124 ± 55†	67 ± 51
OH	56 ± 9	79 ± 25†	22 ± 22‡
CAD	58 ± 5	81 ± 19†	23 ± 16‡
Total MSNA, AU			
YH	1,006 ± 381	5,147 ± 2,379†	4,141 ± 2,523
OH	1,839 ± 557	3,793 ± 1,170†	1,953 ± 1,165‡
CAD	2,372 ± 425*	4,103 ± 996†	1,731 ± 762‡
Action potential indexes			
AP frequency, spikes/min			
YH	216 ± 207	852 ± 491†	636 ± 351
OH	370 ± 191	731 ± 430†	361 ± 303
CAD	447 ± 262	662 ± 301†	215 ± 155‡
AP incidence, spikes/100 hb			
YH	347 ± 340	1,278 ± 669†	931 ± 499
OH	609 ± 298	1,219 ± 738†	610 ± 589
CAD	760 ± 418	1,162 ± 531†	402 ± 312‡

Values are mean ± SD. EE, end-expiratory; MSNA, muscle sympathetic nerve activity; YH, young healthy; OH, older healthy; CAD, coronary artery disease; hb, heart beats; AU, arbitrary units; AP, action potential. *Significantly different from YH baseline value, $P < 0.01$; †Significantly different from baseline, $P < 0.01$; ‡Significantly different from YH delta value, $P < 0.01$.

DISCUSSION

The novel findings of the current work are *1*) compared with young individuals, the ability to increase within-burst firing frequency of already-recruited sympathetic fibers was reduced with aging and CAD; *2*) the capacity of the sympathetic nervous system to recruit subpopulations of previously silent and faster conducting fibers was reduced with aging and lost in CAD; and *3*) the ability to acutely modify synaptic delays and/or central processing times appears preserved with aging and CAD. Taken together, this work supports the hypothesis that cardiovascular disease impairs sympathetic recruitment during apneic stress.

Voluntary apnea represents a robust stimulus for efferent sympathetic outflow through various mechanisms including hypoxia and hypercapnia-induced chemoreceptor activation, removal of the inhibitory influence of lung-stretch receptors, and an increased central drive-to-breathe (17, 37, 38). Early work from single-unit recordings demonstrated that the homeostatic adjustment to apnea involves an increased neural firing frequency and probability, as well as an increase in the incidence of multiple within-burst firing of single axons (22). Our previous work (2, 5, 39), and the results from the current study using a multiunit approach, are in agreement with this finding, at least in YH individuals. Although both OH individuals and CAD patients achieved an elevation in total sympathetic outflow through increased frequency and incidence of AP firing during apnea, the ability to increase the number of APs per sympathetic burst was reduced with healthy aging and lost in CAD patients. Therefore, the impact of CAD appears to be

Downloaded from journals.physiology.org/journal/ajpheart at Univ Western Ontario (129.100.136.165) on September 1, 2022.

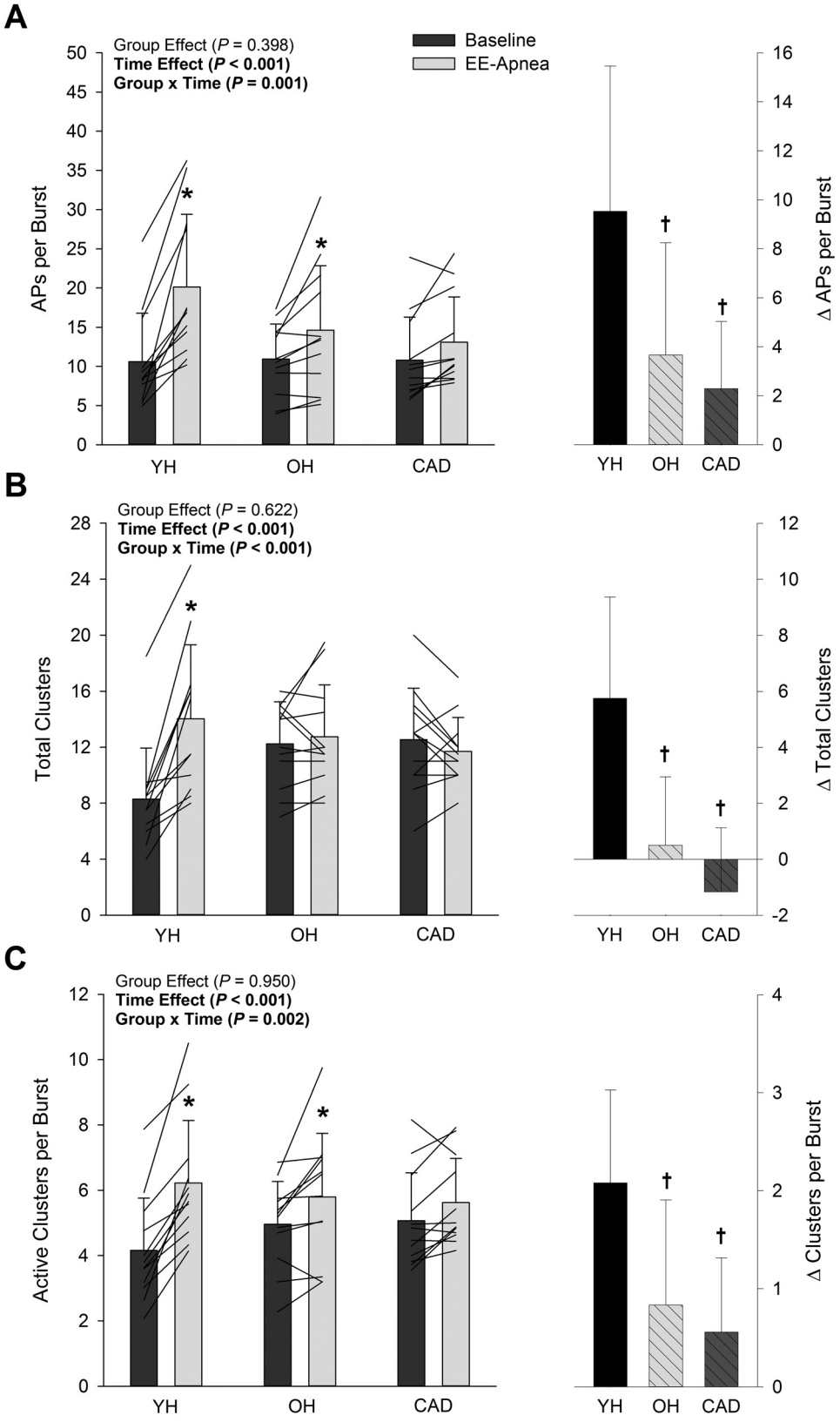

Fig. 4. Action potential (AP) content per burst (*A*), total clusters (*B*), and active clusters per burst (*C*) in young healthy (YH), older healthy (OH), and coronary artery disease (CAD) patients at baseline and during end-expiratory (EE) apnea (left panel; individual lines represent individual data). Right panel represents the absolute delta change from baseline to EE-apnea. *Significantly different from baseline, $P < 0.01$. †Significantly different from YH, $P < 0.01$.

Downloaded from journals.physiology.org/journal/ajpheart at Univ Western Ontario (129.100.136.165) on September 1, 2022.

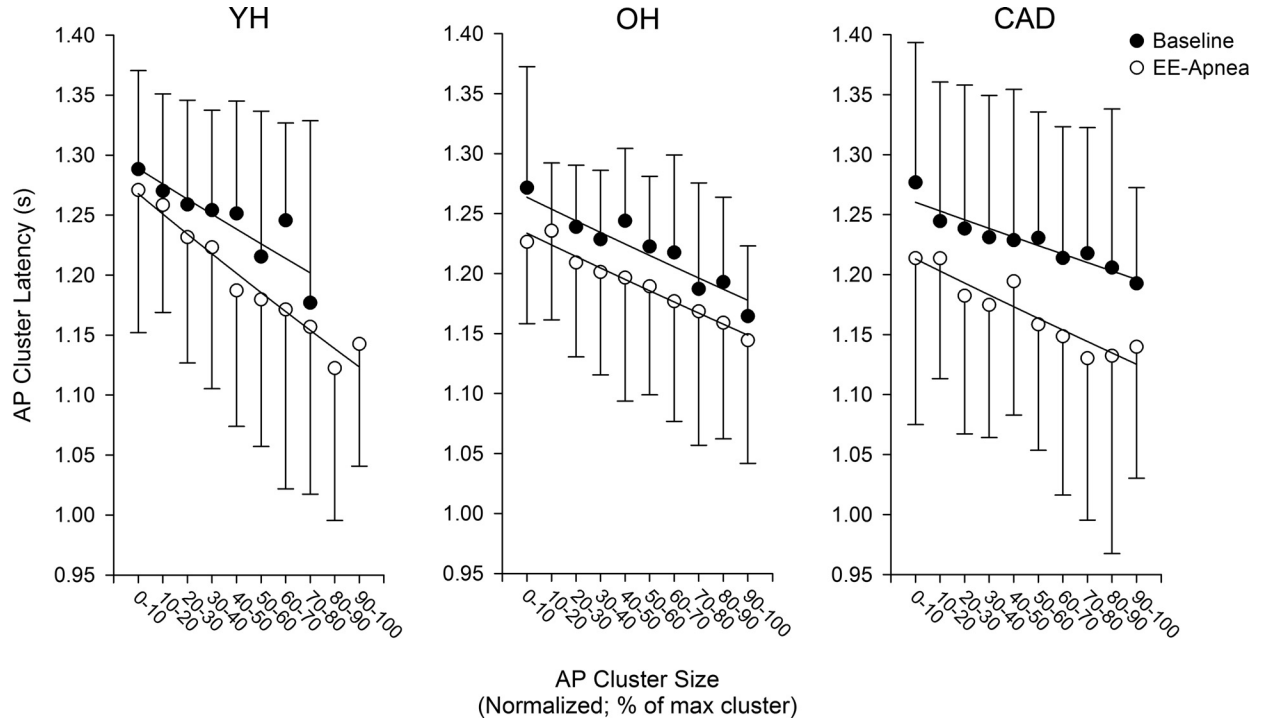

Fig. 5. Action potential (AP) cluster latency as a function of normalized cluster number (i.e., size) at baseline and during end-expiratory (EE) apnea in young healthy (YH; left panel), older healthy (OH; middle panel), and coronary artery disease patients (CAD; right panel).

additive to normal age-related changes in central autonomic integration.

Previously, we observed recruitment of latent subpopulations of larger and faster conducting sympathetic axons during periods of severe autonomic stress, elicited via voluntary apnea (2, 5, 39) and by −80 mmHg lower-body negative pressure (2, 31). However, the current work extends this knowledge to pathological states with known sympathetic dysregulation. In accordance with previous work (24, 25), we show here that older individuals have a reduced capacity to recruit these latent neural subpopulations compared with their young counterparts, while the ability to do so is further reduced and perhaps lost altogether in CAD. The mechanism of this dysregulation is unknown. One possibility is that the elevation in efferent sympathetic outflow at rest observed with healthy aging and cardiovascular disease is, in part, mediated by the additional recruitment of these latent subpopulations, thereby reducing the residual capacity for further recruitment during acute physiological stress. However, the capacity for neural recruitment was not hindered in otherwise healthy, younger subjects with high baseline MSNA (~75 bursts/100 hb) (22), discounting the possibility that a ceiling effect impairs the ability to observe normal recruitment patterns. Furthermore, if these larger axons were already recruited at rest, one may presume that older individuals and CAD patients would have greater AP content per sympathetic burst during baseline resting conditions; however, this was not the case in our study. These observations point to abnormal central features of neural recruitment with healthy aging and perhaps more so with cardiovascular disease, rather than a loss of sympathetic reserve due to elevated resting sympathetic outflow.

Synaptic delay variations and/or altered central processing times appear to exist as a third recruitment strategy used by the sympathetic nervous system to modify efferent sympathetic outflow in the face of physiological challenge (2, 32). The current observations replicate earlier observations (2), in that voluntary apnea caused an acute downward shift in the AP cluster size-latency relationship in YH individuals, such that all APs with similar peak-to-peak amplitudes were recruited with a shorter latency during the reflex-mediated stress. Previous reports indicate that single axons display large latency variations at rest (23), and that reflex latency can change acutely with stress (7, 11). The multiunit approach used here suggests that a systemic and coordinated change in synaptic delay can occur as well. Interestingly, this systemic downward shift in the AP cluster size-latency profile with apnea was preserved with aging, as well as CAD, suggesting that, in contrast to actual recruitment, the option for synaptic delay variations is preserved in these individuals. The location(s) or source of the change in synaptic delay during apnea-induced stress remains unknown, but may be due to the direct activation of the rostral ventrolateral medulla from the nucleus tractus solitarius (20) specific to chemoreceptor activation, and/or the presence of faster conduction velocities within spinal descending pathways specific to chemoreceptor stimulation (~5.5 m/s) vs. baroreceptor activation (~3.3 m/s) (19).

Methodological considerations. Whether the recruitment impairment in OH individuals and CAD patients was due to a smaller reflex stimulus, or to the pathology, cannot be determined specifically from the current analysis. In the context of stimulus strength, variations in the apnea stimulus may have influenced the between-group variations reported in the current study. As mentioned above, the determinants of the apnea autonomic response are not certain and may include the magnitude of chemoreflex stress, loss of lung-stretch afferent activity, or an emotional drive to breathe (17, 37, 38), and

Downloaded from journals.physiology.org/journal/ajpheart at Univ Western Ontario (129.100.136.165) on September 1, 2022.

various factors influence the breakpoint for voluntary apnea (28). In this context, lack of arterial blood gas measures represents a potential limitation of the current study. Although the apnea duration varied within and among groups, they were each of maximal voluntary duration and elicited near-maximal levels of burst probability; therefore, these represent maximal sympathetic efforts. Furthermore, in the current study, EI- and EE-apnea duration correlated poorly with indexes of AP recruitment. While apnea duration related significantly to the total clusters response ($r = 0.554$) to EI-apnea (but not EE-apnea; $r = 0.297$), this was no longer the case when the effects of age and CAD were accounted for. Therefore, at least in our data set, variations in apnea duration are an unlikely determinant of the current observations.

Second, as is commonly practiced (21, 24, 26), CAD patients were studied during their standard pharmacological treatment, and no data exist regarding the effect of medications on sympathetic neural recruitment strategies. However, medication use is a "life-long" therapy for CAD patients, increasing the relevance of studying these participants in the pharmacologically treated state. In addition, all OH individuals studied currently were unmedicated and still displayed impaired central recruitment. If the pharmacological treatment in CAD was causing the further detriment in recruitment observed in CAD vs. OH during EI-apnea, one would expect the same further detriment in recruitment during EE-apnea; however, this was not the case. Taken together, these observations provide evidence to the fact that antihypertensive medications are unlikely to be playing a role in our observed findings.

Furthermore, CAD patients had greater body mass index (BMI) than their YH and OH counterparts, and increased BMI has been known to alter baseline integrated MSNA (33). Whether elevated BMI affects AP recruitment patterns remains unknown; however, in the current study, BMI correlated poorly to all but one index of sympathetic recruitment, suggesting it did not play a role in our observed findings. Nonetheless, when all subjects were pooled, BMI was correlated moderately to the total cluster response to EI- ($r = 0.441$, $P = 0.003$) and EE- ($r = 0.371$, $P = 0.026$) apnea. However, when accounting for age and incidence of CAD, BMI no longer predicted the total cluster response to either apnea. In addition, these aberrant AP recruitment patterns were observed within 2–4 mo of the coronary event, and their persistence will require additional study.

Finally, we acknowledge that the use of only one sympathoexcitatory reflex limits the applicability of the apnea outcomes to other important reflexes, and therefore, future study should assess responses to additional reflex stimuli (i.e., baroreflex, metaboreflex, cold pressor test, etc.) to determine if the observed impairment in central recruitment with aging and cardiovascular disease is specific to apneic stress or a generalized pattern across reflexes.

Summary. Autonomic nervous system dysregulation represents a hallmark of increasing age and cardiovascular disease. Studied primarily under resting conditions, healthy aging and cardiovascular disease are characterized by chronic sympathetic activation, and this state has deleterious consequences for overall health and prognosis. For the first time, the current data indicate that this sympathetic dysfunction extends to the neural coding strategies used by the sympathetic nervous system to respond to acute homeostatic challenge. Specifically, the sympathetic nervous system normally has options to increase the firing of already-recruited axons, recruit latent subpopulations of higher-threshold and faster conducting axons, and modify acutely synaptic delays in response to autonomic arousal. The ability to acutely modify synaptic delays and/or central processing times appears preserved with aging and CAD. However, the ability to increase firing frequency and probability of low-threshold axons is reduced with healthy aging and more so with CAD. Furthermore, the ability to recruit previously silent subpopulations is reduced with increasing age and perhaps lost altogether with CAD. As such, CAD augments the impact of age on recruitment strategies employed by the sympathetic nervous system.

ACKNOWLEDGMENTS

We acknowledge J. Vording and A. Fleischhauer for assistance with this project.

GRANTS

This study was funded by the Canadian Institutes of Health Research Team Grant in Physical Activity, Mobility, and Neural Health (Grant No. 217532; J. K. Shoemaker), an Ontario Graduate Scholarship (T. D. Olver), and a Canadian Institutes of Health Research Doctoral Research Award (M. B. Badrov). J. K. Shoemaker is a Tier 1 Canada Research Chair.

DISCLOSURES

No conflicts of interest, financial or otherwise, are declared by the author(s).

AUTHOR CONTRIBUTIONS

M.B.B., T.D.O., and J.K.S. conception and design of research; M.B.B., S.L., and J.K.S. performed experiments; M.B.B. analyzed data; M.B.B., S.L., T.D.O., N.S., and J.K.S. interpreted results of experiments; M.B.B. prepared figures; M.B.B. and J.K.S. drafted manuscript; M.B.B., S.L., T.D.O., N.S., and J.K.S. edited and revised manuscript; M.B.B., S.L., T.D.O., N.S., and J.K.S. approved final version of manuscript.

REFERENCES

1. **Ashley C, Burton D, Sverrisdottir YB, Sander M, McKenzie DK, Macefield VG.** Firing probability and mean firing rates of human muscle vasoconstrictor neurones are elevated during chronic asphyxia. *J Physiol* 588: 701–712, 2010.
2. **Badrov MB, Usselman CW, Shoemaker JK.** Sympathetic neural recruitment strategies: responses to severe chemoreflex and baroreflex stress. *Am J Physiol Regul Integr Comp Physiol* 309: R160–R168, 2015.
3. **Barman SM, Gebber GL.** "Rapid" rhythmic discharges of sympathetic nerves: sources, mechanisms of generation, and physiological relevance. *J Biol Rhythms* 15: 365–379, 2000.
4. **Barretto AC, Santos AC, Munhoz R, Rondon MU, Franco FG, Trombetta IC, Roveda F, de Matos LN, Braga AM, Middlekauff HR, Negrao CE.** Increased muscle sympathetic nerve activity predicts mortality in heart failure patients. *Int J Cardiol* 135: 302–307, 2009.
5. **Breskovic T, Steinback CD, Salmanpour A, Shoemaker JK, Dujic Z.** Recruitment pattern of sympathetic neurons during breath-holding at different lung volumes in apnea divers and controls. *Auton Neurosci* 164: 74–81, 2011.
6. **Brychta RJ, Shiavi R, Robertson D, Diedrich A.** Spike detection in human muscle sympathetic nerve activity using the kurtosis of stationary wavelet transform coefficients. *J Neurosci Methods* 160: 359–367, 2007.
7. **Coote JH, Macleod VH.** Evidence for the involvement in the baroreceptor reflex of a descending inhibitory pathway. *J Physiol* 241: 477–496, 1974.
8. **Diedrich A, Charoensuk W, Brychta RJ, Ertl AC, Shiavi R.** Analysis of raw microneurographic recordings based on wavelet de-noising technique and classification algorithm: wavelet analysis in microneurography. *IEEE Trans Biomed Eng* 50: 41–50, 2003.
9. **Elam M, Macefield V.** Multiple firing of single muscle vasoconstrictor neurons during cardiac dysrhythmias in human heart failure. *J Appl Physiol* 91: 717–724, 2001.

Downloaded from journals.physiology.org/journal/ajpheart at Univ Western Ontario (129.100.136.165) on September 1, 2022.

10. **Elam M, McKenzie D, Macefield V.** Mechanisms of sympathoexcitation: single-unit analysis of muscle vasoconstrictor neurons in awake OSAS subjects. *J Appl Physiol* 93: 297–303, 2002.
11. **Fagius J, Sundlof G, Wallin BG.** Variation of sympathetic reflex latency in man. *J Auton Nerv Syst* 21: 157–165, 1987.
12. **Ferrigno M, Hickey DD, Liner MH, Lundgren CE.** Cardiac performance in humans during breath holding. *J Appl Physiol* 60: 1871–1877, 1986.
13. **Grassi G, Seravalle G, Dell'Oro R, Mancia G.** Sympathetic mechanisms, organ damage, and antihypertensive treatment. *Curr Hypertens Rep* 13: 303–308, 2011.
14. **Grassi G, Seravalle G, Mancia G.** Sympathetic activation in cardiovascular disease: evidence, clinical impact and therapeutic implications. *Eur J Clin Invest* 45: 1367–1375, 2015.
15. **Greenwood JP, Stoker JB, Mary DA.** Single-unit sympathetic discharge: quantitative assessment in human hypertensive disease. *Circulation* 100: 1305–1310, 1999.
16. **Hagbarth KE, Vallbo AB.** Pulse and respiratory grouping of sympathetic impulses in human muscle nerves. *Acta Physiol Scand* 74: 96–108, 1968.
17. **Hardy JC, Gray K, Whisler S, Leuenberger U.** Sympathetic and blood pressure responses to voluntary apnea are augmented by hypoxemia. *J Appl Physiol* 77: 2360–2365, 1994.
18. **Janig W, McLachlan EM.** Characteristics of function-specific pathways in the sympathetic nervous system. *Trends Neurosci* 15: 475–481, 1992.
19. **Janig W, Szulczyk P.** Conduction velocity in spinal descending pathways of baro- and chemoreceptor reflex. *J Auton Nerv Syst* 1: 149–160, 1979.
20. **Koshiya N, Huangfu D, Guyenet PG.** Ventrolateral medulla and sympathetic chemoreflex in the rat. *Brain Res* 609: 174–184, 1993.
21. **Macefield VG, Rundqvist B, Sverrisdottir YB, Wallin BG, Elam M.** Firing properties of single muscle vasoconstrictor neurons in the sympathoexcitation associated with congestive heart failure. *Circulation* 100: 1708–1713, 1999.
22. **Macefield VG, Wallin BG.** Firing properties of single vasoconstrictor neurones in human subjects with high levels of muscle sympathetic activity. *J Physiol* 516: 293–301, 1999.
23. **Macefield VG, Wallin BG, Vallbo AB.** The discharge behaviour of single vasoconstrictor motoneurones in human muscle nerves. *J Physiol* 481: 799–809, 1994.
24. **Maslov PZ, Shoemaker JK, Dujic Z.** Firing patterns of muscle sympathetic neurons during apnea in chronic heart failure patients and healthy controls. *Auton Neurosci* 180: 66–69, 2014.
25. **Maslov PZ, Breskovic T, Brewer DN, Shoemaker JK, Dujic Z.** Recruitment pattern of sympathetic muscle neurons during premature ventricular contractions in heart failure patients and controls. *Am J Physiol Regul Integr Comp Physiol* 303: R1157–R1164, 2012.
26. **Murai H, Takamura M, Maruyama M, Nakano M, Ikeda T, Kobayashi D, Otowa K, Ootsuji H, Okajima M, Furusho H, Takata S, Kaneko S.** Altered firing pattern of single-unit muscle sympathetic nerve activity during handgrip exercise in chronic heart failure. *J Physiol* 587: 2613–2622, 2009.
27. **Murai H, Takata S, Maruyama M, Nakano M, Kobayashi D, Otowa K, Takamura M, Yuasa T, Sakagami S, Kaneko S.** The activity of a single muscle sympathetic vasoconstrictor nerve unit is affected by physiological stress in humans. *Am J Physiol Heart Circ Physiol* 290: H853–H860, 2006.
28. **Parkes MJ.** Breath-holding and its breakpoint. *Exp Physiol* 91: 1–15, 2006.
29. **Pauletto P, Scannapieco G, Pessina AC.** Sympathetic drive and vascular damage in hypertension and atherosclerosis. *Hypertension* 17: III75–III81, 1991.
30. **Salmanpour A, Brown LJ, Shoemaker JK.** Spike detection in human muscle sympathetic nerve activity using a matched wavelet approach. *J Neurosci Methods* 193: 343–355, 2010.
31. **Salmanpour A, Brown LJ, Steinback CD, Usselman CW, Goswami R, Shoemaker JK.** Relationship between size and latency of action potentials in human muscle sympathetic nerve activity. *J Neurophysiol* 105: 2830–2842, 2011.
32. **Salmanpour A, Frances MF, Goswami R, Shoemaker JK.** Sympathetic neural recruitment patterns during the Valsalva maneuver. *Conf Proc IEEE Eng Med Biol Soc* 2011: 6951–6954, 2011.
33. **Scherrer U, Randin D, Tappy L, Vollenweider P, Jéquier E, Nicod P.** Body fat and sympathetic nerve activity in healthy subjects. *Circulation* 89: 2634–2640, 1994.
34. **Scott DW.** On optimal and data-based histograms. *Biometrika* 66: 605–610, 1979.
35. **Seals DR, Esler MD.** Human ageing and the sympathoadrenal system. *J Physiol* 528: 407–417, 2000.
36. **Shoemaker JK, Badrov MB, Al-Khazraji BK, Jackson DN.** Neural control of vascular function in skeletal muscle. *Compr Physiol* 6: 303–329, 2016.
37. **Somers VK, Mark AL, Zavala DC, Abboud FM.** Influence of ventilation and hypocapnia on sympathetic nerve responses to hypoxia in normal humans. *J Appl Physiol* 67: 2095–2100, 1989.
38. **Steinback CD, Breskovic T, Frances M, Dujic Z, Shoemaker JK.** Ventilatory restraint of sympathetic activity during chemoreflex stress. *Am J Physiol Regul Integr Comp Physiol* 299: R1407–R1414, 2010.
39. **Steinback CD, Salmanpour A, Breskovic T, Dujic Z, Shoemaker JK.** Sympathetic neural activation: an ordered affair. *J Physiol* 588: 4825–4836, 2010.
40. **Tukey JW.** *Exploratory Data Analysis*. Reading, MA: Addison-Wesley, 1977.

Downloaded from journals.physiology.org/journal/ajpheart at Univ Western Ontario (129.100.136.165) on September 1, 2022.